THE ASTROPHYSICAL JOURNAL, 280:41–50, 1984 May 1

OPTICAL IMAGING OF 78 QUASARS AND HOST GALAXIES

J. B. HUTCHINGS[1] AND D. CRAMPTON[1]
Dominion Astrophysical Observatory

AND

BRUCE CAMPBELL
Canada-France-Hawaii Telescope Corporation
Received 1983 June 21; accepted 1983 October 17

ABSTRACT

Results are presented of $\sim 1''$ resolution optical imaging of 78 QSOs which have redshifts from 0.0 to 0.7. Data in *B* and *R* colors are available for approximately half of the sample. Fuzz, presumably a host galaxy, is clearly resolved in all but seven objects, and the study examines the colors, morphologies, and luminosities of these host galaxies, as well as the colors and luminosities of the unresolved nuclei. The sample contains nearly equal fractions of radio, optically and X-ray selected objects, about uniformly distributed in luminosity and redshift. No significant differences are apparent among these discovery types, in most parameters. The radio selected QSOs are ~ 1.7 mag more luminous and reside in galaxies ~ 1.5 mag more luminous than the other QSOs, and the radio luminosity shows some correlation with host galaxy luminosity. The QSO nuclear luminosities are correlated, with a slope 1.6, with the host galaxy luminosity, and are, on the average, 0.6 mag brighter. About one-third of all QSOs appear to be interacting with another galaxy, while over one-quarter clearly lie in small compact groups or clusters of galaxies. Over 40% of the host galaxies show some spiral characteristics, the remainder having undetermined morphology. These fractions are not mutually exclusive. There is no positive evidence of ellipticals among the host galaxies. The photometric colors of QSOs reflect the nuclear to galaxy luminosity ratio, bright nuclei objects being bluer. Other correlations and properties discussed are axial ratios and scale lengths of host galaxies, and X-ray and radio luminosities.

Subject heading: quasars

I. INTRODUCTION

We have reported in earlier publications (Hutchings *et al.* 1981, 1982; Hutchings, Campbell, and Crampton 1982; Hutchings and Campbell 1983; hereafter referred to as Papers I–IV) some of the results of optical imagery of low-redshift QSOs with the prime focus camera of the Canada-France-Hawaii telescope (CFHT). These earlier papers have discussed smaller samples, particular aspects of the work, or individual objects of interest. In this paper we present and discuss all the results of measurements on a sample of 78 objects, which includes our previously observed objects. The objects range in redshift up to $z \sim 0.6$ and cover, as uniformly as was practical, luminosity over ~ 4 mag in three discovery-type categories: radio, optical, and X-ray. The sample thus represents a moderately good statistical basis for general descriptions of QSOs and their host galaxies. A similar study involving some of the same objects is being undertaken by Wyckoff, Wehinger, and Gehren (1981) and Wyckoff *et al.* (1983). Stockton (1982) and Tyson, Baum, and Kreidl (1982) have recently published high-resolution imagery of some QSOs, while spectroscopic observations of the nebulosity around low-luminosity quasars by Boroson, Oke, and Green (1982) and Balick and Heckman (1983) indicate that most of the underlying galaxies are probably spirals.

This paper presents the results of the overall program. Maps, intensity plots, and individual comments on the objects will be published elsewhere.

II. DATA

Our complete data set comprises about 350 direct photographic plates with IIIa emulsions, at $\sim 14'' \text{ mm}^{-1}$ scale. The majority of these were taken with the CFHT ITT single-stage 90 mm image tube, and usually four sky-limiting plates were taken of each field with centers slightly displaced from each other to minimize the "chicken wire" effect of the fiber optic output window. These were summed digitally before analysis. In the case of very bright objects, a short exposure was also taken to record an unsaturated image of the QSO nucleus. The sum of four image tube exposures has similar signal-to-noise to the earlier single sky-limiting direct exposures. Table 1 lists all the objects observed, their principal characteristics, and measured quantities.

The image quality was remarkably good and uniform over several observing runs. Figure 1 shows histograms of the FWHM and mean profiles of point spread functions in the two colors derived from field stars. The full width at $\sim 1\%$ of the peak of the point spread function, a more important quantity in this type of work, was $\sim 1''.5$ in most cases. The uniformity of the seeing is an important feature of the sample, but corrections were derived and applied in some cases for seeing differences.

The data acquisition and reduction techniques are described in Papers I–III, and we have attempted to keep our

[1] Visiting Astronomer, Canada-France-Hawaii Telescope, operated by the National Research Council of Canada, the Centre National de la Recherche Scientifique of France, and the University of Hawaii.

TABLE 1

IMAGING DATA FOR ALL QSOs

QSO PROPERTIES									RED IMAGE DATA								BLUE IMAGE DATA								COLOR
Name		z	B	V	R	L_X	L_R	Morphology	"	PL	L_N/L_F		M_G	M_N	b/a(mag)	Sc.L.(kpc)	"	PL	L_N/L_F		M_G	M_N	b/a(mag)	Sc.L(kpc)	$(B-V)_o$
1	2	3	4	5	6	7	8	9	10	11	12	13	14	15	16	17	18	19	20	21	22	23	24	25	26
0007+106(I11Zw2)	O	0.09	16.0	15.4	(15.0)	-	7.4	S(arm), G	1.1	24.1	4.1	2.6	-20.9	-21.8	.77,.69(23)	1.9,(5.7),1.7C	0.8	26.6	35	42	-17.5	-21.0	.84,.70(25)	(4.9)	0.1N,1.1G,0.2K
0037+061	X	0.06	17.9	17.0	(16.7)	42.8	<4E-3	S(arm, blue)	1.3	23.9	0.5	0.33	-19.4	-18.5	.75,.70(23)	1.4	1.5	25.7	0.83	0.44	-18.3	-17.1	.67,.67(24)	20	0.3N,1.1G,0.0K
0132+077(PHL1049)	O	0.15	17.9	17.3	(16.8)	-	<.023	S?(very blue)	1.2	23.9	0.4	0.22	-21.4	-19.6	.79,.81(23)	2.0	1.5	25.0	0.90	0.32	-20.8	-19.0	.81,.83(24)	2.9	0.3N,0.3G
0134+033(PHL1070)	O	0.08	17.9	17.6	(17.3)	42.1	<6E-3	S?(bar)	0.9	24.8	1.4	1.4	-18.8	-19.1	.96,.74(23)	2.3,0.7C	1.6	26.9	7.5	5.0	-17.6	-18.9	1.1,.81(24.6)	2.5,1.2C	0.2N,1.1G,2.3C
0147+089(PHL1186)	O	0.27	17.4	17.4	(17.4)	-	-	S? I?	1.0	23.4	3.2	0.9	-22.1	-21.8	.83,.94(23)	1.7									
0148+090(PHL1194)	O	0.30	17.4	17.5	(17.5)	-	-	-	1.0	23.7	9.0	2.5	-21.6	-22.4	.90,1.0(23)	1.9									
0214-033	X	0.33	(17.0)	16.8	(16.6)	43.7	-	-	0.9	26.0	50	15	-20.7	-23.7	.84,1.0(23)	-									
0225+3120	X	0.06	17.5	16.8	(16.6)	42.8	<2E-3	S(barred)	1.6	25.6	1.1	1.5	-18.8	-19.1	1.3,.61(23)	2.0	1.6	27.0	1.8	1.5	-18.2	-18.2	1.0,.57(24)	1.5	0.7N,0.7G
0241+622	X	0.04	17.8	16.4	(15.4)	-	0.48	S(arms)	1.5	25.3	6.4	8.4	-20.9	-23.1	.75,.73(23)	0.8	1.1	25.8	9.0	10.0	-20.3	-22.6	.55,.68(24)	0.8	0.1N,0.7G,0.3K
0242-387	O	0.12	(18.2)	17.8	(17.4)	-	-	S?(bar)	1.0	24.6	1.2	0.9	-19.7	-19.7	.80,.74(23)	0.9									
0351+026	X	0.04	17.8	16.3	(15.1)	42.6	<2E-3	S,I,H	0.8	24.0	1.5	1.3	-21.9	-22.2	.62,.66(21.5)	1.2,1.0C	0.9	25.8	3.1	3.2	-20.5	-21.6	.60,.64(74)	1.3,1.1C	0.2N,0.9G,0.4C
0357+1046	X	0.18	17.1	16.8	(16.7)	43.8	<0.02	S?Ir	1.1	24.9	18	12	-21.1	-22.0	1.0,1.0(23)	(5.9)									
0607-157	R	0.32	(18.2)	18.0	(17.8)	-	-	I? G	1.4	25.4	∞	-	-	-22.4	-	-,1.7C									
0721+690	X	0.11	(17.0)	16.8	(16.6)	43.2	-	S?	1.5	23.5	6.8	3.6	-19.5	-20.8	.80,.73(23)	2.0									
0742+318(4C31.30)	R	0.46	(16.2)	16.0	(15.8)	-	-	I??	1.1	24.0	∞	-	-	-25.5	-	-									
0752+258(01287)	R	0.45	(17.2)	17.0	(16.8)	-	135	-	1.4	24.1	41	7	-22.6	-24.3	.90	3.2									
0754+3928	X	0.10	14.7	14.4	(14.2)	43.5	0.034	-	1.1	24.6	86	56	-18.9	-23.2	.74,.89(23)	1.6									
0840+503(U10)	O	0.30	(18.3)	18.1	(17.9)	-	-	S(bar?)	0.7	24.8	4.0	1.6	-21.5	-21.7	.71,.64(23);61(22)	1.7(4.0)									
0844+377	X	0.45	17.2	17.7	(17.8)	44.2	<0.20	Ir,I?	1.0	23.9	20	3.0	-22.4	-23.1	.96,.86(23)	2.8,2.4C,2.4C									
0845+378	X	0.31	17.6	17.9	(18.0)	43.6	<0.10	H	1.0	24.7	2.4	0.9	-21.8	-21.4	.87,.92(23)	2.8,3.0C									
0846+100(4C09.31)	R	0.37	19.4	19.2	(19.0)	-	0.82	Ir,G,I?	1.0	25.9	12.3	5.5	-20.1	-21.5	.61,1.0(23)	2.9,2.9C,2.9C									
0851+202(0J287)	R	(0.31)	14.4	14.0	(13.9)	-	-	-	1.0	23.4	>100	>23	>-23.1	-26.3	-	-									
0906-091	X	0.13	(18.5)	18.3	(18.2)	42.2	-	G,I??F	1.0	24.1	5.4	3.3	-18.3	-19.5	.76,1.0(23)	1.1,1.1C									
0906+484	O	0.12	16.5	16.1	15.9	-	-	S(barred)	1.5	25.3	4.6	2.1	-20.8	-21.5	1.4,.92(23),.66(22)	3.1,3.4C	1.0	25.0	2.8	1.6	-20.9	-20.9	1.3,.79(23)	4.5,5.6C	0.4G,0.2C
0957+227(4C22.25)	R	(0.10)	18.3	18.0	(17.9)	-	2.0	I	1.0	24.0	4.9	3.2	-18.2	-19.4	1.0	1.1,0.9C									
1011-282(0L-219)	R	0.25	(15.9)	15.7	(15.5)	-	2.3	H	1.1	23.5	44	13	-21.5	-24.0	.74,1.0(22.5)	-									
1020-103(0L-133)	R	0.20	(16.7)	16.5	(16.3)	-	18.0	-	0.9	25.1	35	23	-19.5	-22.8	.88,.92(24),1.0(23)	3.5									
1031+5822	X	0.25	19.2	18.7	(18.2)	43.5	<0.034	G,I??,F	0.9	24.8	0.14	0.07	-21.6	-18.4	.43,1.0(24)	2.0,2.0C,2.0C									
1059+730	X	0.09	16.4	14.7	(14.0)	43.1	<8E-3	S,I??,G	1.0	22.8	1.3	0.57	-22.8	-23.0	.42,.37(22),51(21)	1.3,1.5C	1.4	25.4	1.0	0.57	-20.8	-21.7	.42,.48(24)	1.2,1.6C	G=N+0.2,C=N
1139+1040	X	0.15	20.0	19.0	(18.5)	43.6	-	S,I?	1.0	25.2	0.33	0.28	-19.6	-18.1	.96,.90(24),.67(23)	3.6,3.6C									
1203+011	R	0.10	(18.4)	18.2	(18.0)	-	1.6	I?G,F	0.8	24.5	∞	-	-	-19.5	-	-,0.6C									
1216+069	O	0.33	15.7	(15.3)	(15.1)	-	-	H	1.5	26.0	27	6.5	-23.4	-25.0	.83,1.0(25)	5.0(10)									
1225+0858	X	0.09	17.0	16.6	(16.4)	43.3		S?Ir	1.3	22.4	1.2	0.47	-20.5	-19.6	1.0	1.9	1.1	24.4	2.0	1.1	-19.9	-19.5	1.0,.86(22.5)	1.7	0.2N,0.6G
1225+0930	X	0.73	19.4	18.7	(18.1)	44.2	-	-	1.3	22.4	∞	-	-	-24.4	-	-									
1226+1336	X	0.15	17.9	17.2	(16.9)	43.1	-	S?I??	1.0	24.1	3.2	1.9	-20.3	-20.9	.70,1.0(23)	2.1									
1227+1403	X	0.10	18.1	17.4	(17.1)	43.2	-	I?F?	1.0	24.3	1.5	1.1	-19.7	-19.7	1.0,1.0(23)	2.1,2.1C									
1229+204(TON1542)	O	0.06	15.6	15.3	(15.1)	-	<4E-3	S(barred),I	1.0	24.9	2.2	2.0	-20.0	-20.8	.94,.64(23)	1.2,2.5C	1.2	25.4	3.5	3.2	-19.4	-20.4	.90,.62(23)	1.1,2.9C	0.2N,0.5G,-0.1C
1248+337(BSO 2)	O	(0.19)	18.9	18.6	(18.4)	-	-		0.9	24.1	∞	-	-	-20.7	-	-	1.0	24.3	∞	-	-	-20.3	-	-	-	-
1254-333	R	0.19	18.8	18.3	(18.0)	-	<.036	H	1.3	25.3	2.1	1.5	-20.1	-20.4	.55,1.0(24)	1.3	1.6	27.0	<150	<56	-16.0	-20.3	-	-	-
1257+35	X	0.32	19.8	19.8	(19.8)	-	-	H	1.0	25.2	1.9	0.8	-20.1	-19.5	.78,1.0(24)	2.2									

TABLE 1—*Continued*

Name		z	B	V	R	L_X	L_R	Morphology	"	PL	L_N/L_F		M_G	M_N	b/a(mag)	Sc.L.(kpc)	"	PL	L_N/L_F		M_G	M_N	b/a(mag)	Sc.L(kpc)	$(B-V)_o$
1	2	3	4	5	6	7	8	9	10	11	12	13	14	15	16	17	18	19	20	21	22	23	24	25	26
1300-361(B234)	O	0.06	18.4	17.5	(17.2)	-	-	Ir,I?,G	0.9	24.2	0.47	0.40	-18.7	-17.7	.80,1.0(23)	0.9,0.9C,0.4C									
1302-102(OP-106)	R	0.29	15.0	14.9	(14.8)	-	100	H	1.2	24.1	20	4.7	-23.6	-25.0	-	(3.8)	1.4	24.0	∞	-	-	-25.1	-	-	-
1351+640	O	0.09	15.2	14.8	(14.7)	42.5	-	G	1.0	24.0	13	8.8	-20.2	-22.5	.84,1.0(23)	3.0	1.3	26.1	38	25	-19.1	-22.1	1.0	2.9	0.9G
1352+1820	X	0.15	15.6	15.5	(15.4)	44.3	<0.014	H	1.0	23.2	18	7.5	-20.7	-22.8	.61,1.0(22.5)	2.1									
1400+162(4C16.39)	R	0.24	(16.7)	16.5	(16.3)	-	7.5	I?,G	0.6	23.0	13.6	3.7	-21.8	-22.8	.66,1.0(22)	2.2,1.8C									
1425+267(TON202)	O	0.37	15.7	(15.5)	(15.3)	-	-	Ir,I?,H	1.3	23.9	10	1.0	-25.0	-24.7	.85,.78(23)	6.0,3.7C,2.7C									
1510-089	R	0.36	16.7	16.5	(16.3)	-	-	-	0.9	23.8	53	11.2	-21.9	-24.1	-	-,2.2C									
1525+1551	X	0.23	17.3	17.2	(17.1)	44.0	<.053	-	1.0	23.7	17	6.1	-20.5	-22.2	1.0	1.3.									
1525+227(OR241)	R	0.25	16.2	16.4	(16.4)	-	2.7	I?	0.8	24.0	18	6.4	-21.3	-23.0	.86,1.0(23)	(9.9)									
1557+272	X	0.07	17.2	16.3	(16.0)	42.5	<5E-3	S,I?	-				-	-	-	-	0.8	26.9	12.2	8.0	-17.5	-19.5	.71,.75(25)	2.0	-
1602+2410	X	0.09	17.7	17.1	(16.8)	42.9	<9E-3	S	0.9	24.9	0.9	0.9	-19.9	-19.7	.62,.68(23)	1.8	1.0	26.2	3.0	3.2	-18.6	-19.4	.63,.61(24)	1.9	0.4G
1606+291	O	(0.28)	(19.8)	19.5	(19.2)	-	-	G	0.8	24.3	1.1	0.37	-20.1	-19.9	.68,1.0(23)	1.6,1.6C	1.2	25.1	2.2	0.56	-19.5	-19.5	.60,1.0(24)	1.8	G=N+0.7
1641+399a(3C345)	R	0.60	16.3	16.0	(15.9)	-		I?,G	0.7	25.3	270	39	-23.0	-26.2	.75,1.0(24)	(7.6),2.0C									
1641+399b	X	0.59	18.7	19.3	(19.3)	44.0	<0.35	G	0.7	23.7	2.1	0.18	-23.3	-20.6	.68,1.0(23)	2.4									
1700+518	O	0.29	15.4	(15.2)	(15.0)	-	-	F?	1.4	24.1	>30	>15	-22.2	-24.9	1.0	-									
1704+608a(3C351)	R	0.37	15.4	15.3	(15.2)	44.4	-	H	1.0	23.4	26	4.0	-24.2	-25.3	.82,1.0(22)	(4.0)	1.1	24.4	80	14	-24.1	-25.4	.70,.83(23)	(6)	0.6G
1704+608b	X	0.08	18.9	17.7	(17.3)	42.0	<6E-3	S?H	1.0	23.4	0.42	0.21	-19.5	-17.7	.76,.83(22)	1.6	1.1	24.9	0.50	0.33	-18.1	-16.5	.76,.71(24),.91(23)	1.1	1.0N,1.4G
1725+044	R	0.29	(18.5)	18.2	(17.9)	-	67	I?G	0.8	23.9	6.9	2.0	-21.2	-21.7	.69,.83(23)	1.5,1.5C									
1747+6836	X	0.06	17.1	16.5	(16.0)	43.0	<2E-3	S,Ir,I,G	1.0	22.2	0.38	0.32	-20.1	-18.8	.5(23),.4(22)	1.2,1.4C,1.0C	0.8	24.0	3.3	1.7	-18.4	-18.7	1.0,.40(23)	1.7(6),	0.7N,0.3K,1.3C
1803+676	O	0.14	(16.2)	16.0	(15.8)	43.8	<0.02	Ir	0.9	24.7	36	26	-18.6	-22.3	.72(24)	(5.6),0.8C								1.7C,0.6C	
2130+099(II Zw136)	O	0.06	14.9	14.6	(14.4)	-	<4E-3	S	1.0	24.8	2.6	2.6	-20.6	-21.5	.46,.40(23),.46(22)	1.5,(4.0)	1.1	24.6	164	10.5	-19.0	-21.3	.53,.70(23)	1.8	0.6G,0.0K
2135+147(OX-158)	R	0.20	15.6	15.4	(15.3)	44.6	5.0	I,G	0.8	23.7	8.9	3.7	-22.2	-23.5	1.0,1.0(23)	1.4,1.4C	0.9	25.1	100	45	-20.3	-23.5	1.0,1.0(24)	-,1.8C	0.1N,0.6K,0.9C
2141+175(OX169)	R	0.21	15.7	15.5	(15.3)	43.6	12.3	S?,F	0.9	23.6	14	4.6	-22.2	-23.7	.4,.8(23)	1.5,(3.4)	1.0	25.0	50	21	-21.2	-23.6	.73,.76(23)	2.8(4.6)	0.3G
2201-211	O	(0.23)	(20.0)	19.8	(19.6)	-	-	-	1.2	26.9	∞	-	-	-19.8	-	-									
2201+315(4C31.63)	R	0.30	(15.7)	15.5	(15.3)	-	135	I?	1.0	24.4	9.8	3.3	-23.5	-24.5	.5,.8(23)	6.7	1.1	24.1	175	44	-21.8	-24.5	.68,.82(23)	-	G=N+1.4
2205-167	O	0.16	(19.5)	19.3	(19.1)	-	<.086	Ir,F	0.8	26.0	2.6	3.0	-18.2	-19.2	.76,.76(23)	1.7	1.0	26.0	3.4	2.6	-18.5	-18.8	1.0,1.0(25)	(4)	-
2205-203	O	0.26	(19.7)	19.5	(19.3)	-	<4E-3	H	1.0	23.5	∞	-	-	-20.5	-	-									
2206-197	O	(0.20)	(20.0)	19.7	(19.5)	-	-	Ir,F	1.0	23.8	2.2	0.98	-18.6	-19.1	.63	2.5									
2209-207	O	(0.25)	(19.6)	19.4	(19.2)	-	-	Ir,F	0.9	24.7	>8.6	>4.0	-19.0	-20.2	-	-									
2215-037	X	0.24	17.2	17.2	(17.2)	43.9	<.058	S?I?	1.0	24.2	27	11	-19.9	-22.2	.83,.71(23)	2.5,2.7C	1.1	24.4	26	7.9	-21.1	-22.2	1.2,.87(23)	3.4,3.4C	0.0N,0.0G,1.0C
2217+08NE(4C08.66)	R	0.62	(19.5)	(18.6)	18.1	-	10.5	G	0.9	22.9	2.1	0.12	-24.8	-21.7	1.0	2.5									
2217+08SW	R	0.22	(18.5)	17.6	(17.0)	-	0.33	-	0.9	22.9	0.80	0.22	-22.3	-20.5	.82,1.0(22)	2.6									
2247+140(4C14.82)	R	0.24	(17.2)	17.0	(16.8)	-	70	-	0.9	24.6	6.3	3.0	-21.5	-22.4	.63,.78(23)	2.6									
2251-178	X	0.07	15.0	14.4	(14.2)	44.4	.016	I?G,H	0.8	23.7	1.4	1.0	-21.8	-21.7	1.0,1.0(23)	3.7,1.1C	1.0	27.0	2.4	4.0	-20.3	-21.5	1.3,1.1(25),.85(23)	3.0,0.9C	0.7N,1.1G,1.0C
2251-1751	X	0.07	17.4	16.5	(16.3)	42.7	<2E-3	S(barred)I,G	0.8	23.8	0.29	0.20	-20.3	-18.5	.65,.54(23).46(22)	1.9,0.6C	1.0	25.2	0.42	0.36	-19.2	-17.8	1.2,.54(24),.40(23)	1.9,0.8C	0.6N,0.7G,0.3K
2305+187(4C18.68)	R	0.31	17.1	16.5	(16.1)	-	4.8	Ir,G,I?	1.0	23.8	0.8	0.23	-24.2	-22.3	.83,.67(22)	3.8,2.1C,2.0C,3.9C	1.0	24.0	4.3	0.87	-23.9	-22.3	.65,1.0(23)	3.0,2.9C	0.1N,1.4G,1.0C
2318+049(02031)	R	0.63	(19.2)	19.0	(18.8)	-	-	-	1.0	25.1	48	5.8	-22.1	-23.2	-	-									
2331-240(0Z252	R	0.05	(17.0)	17.0	(16.7)	-	2.2	-	1.5	23.8	0.57	0.44	-18.8	-17.9	.87,.86(23)	1.7,(1.0)	1.3	25.0	1.0	0.52	-18.3	-17.4	.78,.92(24),.80(23)	2.4,1.7C	G=N+0.5

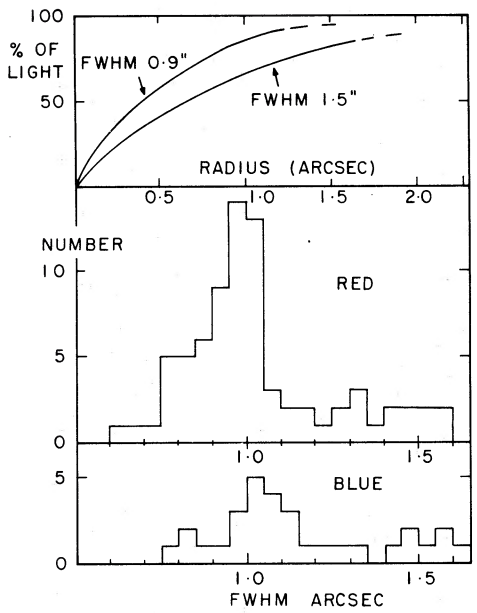

FIG. 1.—Point image data. Upper panel shows percentage of encircled intensity with radius for two typical images. 0".9 is average and 1".5 is worst case. Lower panels show histograms of FWHM for all QSO images in red and blue light.

procedures uniform throughout. Many of the earlier data have been reprocessed with the current software package to ensure uniformity and format compatibility. Thirty-one of the 78 objects were observed in the blue ($\sim B$ band) while 77 were observed in the red ($\sim R$ band). Three of the objects were also observed with a 6070 Å narrow band (175 Å FWHM) filter.

The principal measurements made were of the resolved and unresolved luminosity after subtraction of the point spread function to achieve the best exponential fit to the azimuthally averaged luminosity profile of the resolved part. Axial ratios were measured for the resolved isophotes over as large a range of intensity as possible, and those levels were converted to magnitudes per square arc second using the published magnitude of the QSO as reference. Where two-color data were available, colors were determined for the resolved and unresolved components, and intensity plots were made of color-differenced pictures. In many cases, similar measurements were made on neighboring galaxies.

The luminosity and redshift distributions of the objects in our sample are shown in Figure 2. The principal selection effects involve the shortages of low-redshift radio selected objects and high-luminosity optical objects. As discussed below, these deficiencies may be intrinsic ones to some extent, rather than artifacts of the selection procedure.

As in earlier papers, we have used the cosmological parameters $H_0 = 100$ km s^{-1} Mpc^{-1}, $q_0 = 0$ throughout.

III. CORRECTIONS TO THE MEASURES

a) Redshift, Plate Limit, and Seeing Effects

In Paper II a procedure was derived for correcting the observed fraction of unresolved luminosity for distance effects. We have rederived this correction, and have also derived empirical corrections to remove the effects of differing point spread functions (seeing) and plate limiting magnitudes.

For the redshift correction, the procedure involves selecting a few objects of low redshift having well-determined luminosity profiles and "removing" them to higher redshift values, with appropriate scale factors, intensity ratios, point spread functions, and limiting magnitudes. This was repeated with five low-z QSOs, several classical Seyferts, and a few completely artificial profiles similar to those observed. The results are remarkably similar, and the exponential correlation shown in Figure 3 was adopted and applied to all measured values of the ratio of nuclear to fuzz luminosity, L_N/L_F. The slope of the logarithmic relationships is close to that indicated by the raw data themselves. There is a difference between this correction and that derived in Paper II, which is mainly due to the application of additional corrections (see below), making the procedure an iterative one. A part of the difference is also due to the fact that some of the older

Table 1 Notes, by Column Number

1. Names are as published and consequently inconsistent in declination nomenclature convention.
2. Discovery by X-ray, radio, optical observation.
3. Redshift to 2 significant figures. Values in parentheses are uncertain.
4–6. Apparent magnitudes. Values in parentheses derived using the other two or mean QSO colors.
7. Log of (*Einstein* IPC) X-ray luminosity in ergs s^{-1} for $H_0 = 100$ km s^{-1} Mpc^{-1}.
8. 6 cm core radio luminosity in "units" of mJy · z, using VLA peak intensities only (Gower 1983).
9. QSO morphology summary; S = spiral, I = interacting with companion galaxy, G = group or cluster member, Ir = irregular shape, H = halo or broad tail, F = filament or jet.
10, 18. Point spread function FWHM in arcsec.
11, 19. Plate limit: lowest measured contour in mag arcsec^{-2}.
12, 20. Ratio L_N/L_F of unresolved (nuclear) to resolved (fuzz) luminosity as measured.
13, 21. Corrected L_N/L_F to standard magnitude limit, redshift, and image resolution.
14, 22. Absolute magnitude of QSO host galaxy for $H_0 = 100$ km s^{-1} Mpc^{-1}, $q_0 = 0$, based on corrected L_N/L_F.
15, 23. As previous column for QSO nucleus.
16, 24. Axial ratio b/a for contour at plate limit (cols. [11], [19]). Other values at levels of mag arcsec^{-2} given in parentheses.
17, 25. Scale lengths of azimuthally averaged images in kpc. C denotes QSO companion galaxy. Values in parentheses refer to outer QSO halo.
26. Mean $B-V$ colors corrected to zero redshift, for QSO nuclei (N), host galaxies (G), and companion galaxies (C).

NOTE.—X-ray sources and luminosities from Grindlay *et al.* 1981; Kriss and Canizares 1982; Chanan, Margon, and Downes 1982, 1983; Zamorani *et al.* 1982; Tananbaum 1982. Radio luminosities from Paper II, Gower 1983; Hintzen, Ulvestad, and Owen 1983; Kriss 1982; Chanan, Margon, and Downes 1983.

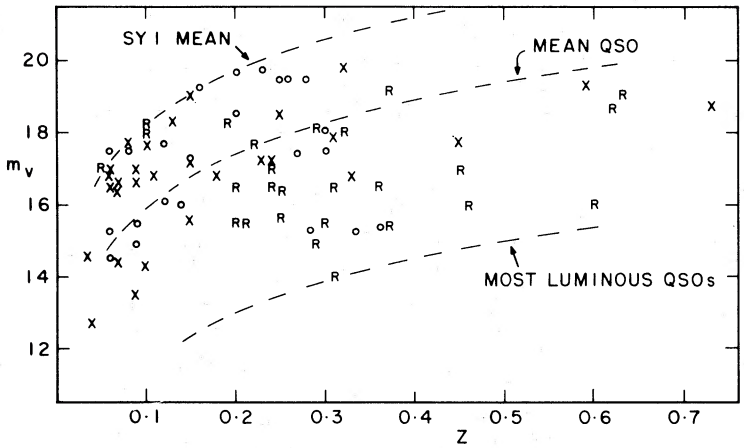

FIG. 2.—Distribution of sample objects in (total) luminosity and redshift. R, X, O denote QSO discovery type: radio, X-ray, and optical. Dashed lines represent constant luminosity typical of mean of 30 Sy 1 galaxies, all Hewitt and Burbidge (1980) $z = 0.1$–0.3 QSOs, and the highest luminosity QSOs. Extinction and redshift corrections have been applied to four objects discussed in the text.

data were reprocessed with an improved calibration to deeper limits.

The dependence of the L_N/L_F ratio on the point spread function and on the limiting magnitude were modelled in a similar way. The results are shown in the lower panels of Figure 3. In these cases the amplitudes of the variation of these quantities in our data are small, so the corrections are also small.

The measured L_N/L_F ratios were corrected to zero redshift, to the 0.9 arcsec FWHM point spread function shown in Figure 1, and to limiting magnitudes $R = 24$ mag arcsec^{-2} and $B = 25$ mag arcsec^{-2}. These latter three values are close to the mean for all objects.

In most cases the plate limits were derived from the published QSO magnitudes (see § IV*a* discussion). Since many QSOs show some variability, this will introduce a random error into the measurements. In a few extreme cases, where it was estimated that the QSO magnitudes must have changed by ~ 1 mag, a revised value was adopted based on the limiting magnitude of exposures taken under similar conditions.

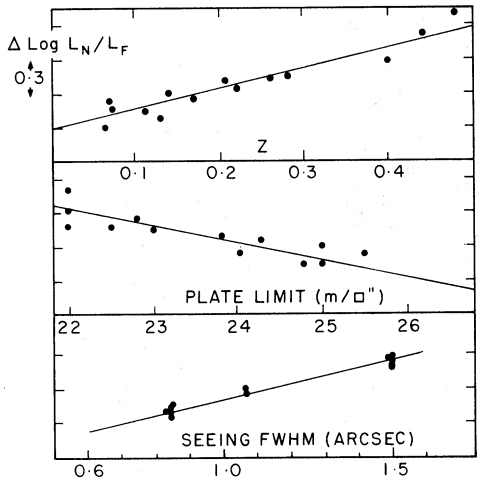

FIG. 3.—Corrections to resolved luminosity fraction for redshift, limiting magnitude, and point spread function (seeing). Points are empirical determinations from well-defined profiles, and lines are adopted relationships. Standard correction is to $z = 0$, 24 mag arcsec^{-1} red, 25 mag arcsec^{-1} blue, 0.″9 FWHM.

b) K-Corrections

In deriving absolute magnitudes for QSO nuclei and underlying galaxies, separate *K*-corrections were applied since their spectral energy distributions are quite different. The values given by Sandage (1973) for the appropriate color were used for the galaxies. Although the type of underlying galaxy is unknown, the differences in the corrections due to incorrect types are small compared to other uncertainties. If the fuzz is not a fairly normal galaxy, this of course may be in error, but in most cases only by a few tenths of a magnitude. For the nucleus, a mean QSO energy distribution was compiled from published *UBV* photometry of the highest luminosity objects in the Hewitt and Burbidge (1980) catalog. These (as this paper confirms) are dominated by their nuclear components, and all have similar energy distributions. Published infrared measurements (Gezari, Schmitz, and Mead 1982) were used to extrapolate beyond 5500 Å. The resulting *K*-corrections for QSO nuclei in *B* and *R* are shown in Figure 4.

c) Foreground Extinction

Corrections were made, in the few cases necessary, for foreground Galactic extinction using the cosecant law (Sandage 1972). There are three very red QSOs. The object 0241+622 is a low-latitude object which is reddened by ~ 1.4 mag (Paper II). The nucleus of 0351+026 is apparently affected by local reddening (Paper III), and so a correction is made only to the nuclear magnitudes. The edge-on appearance of 1059+730 suggests that it, too, may be locally obscured, and so a correction was applied only to the nuclear magnitudes.

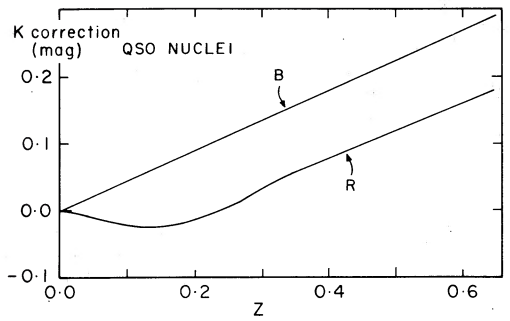

FIG. 4.—*K*-corrections used for QSO nuclei in deriving absolute magnitudes.

IV. NUCLEAR AND HOST GALAXY ABSOLUTE MAGNITUDES

a) Luminosity Ratios

For all resolved objects, we measured the resolved and unresolved components down to the plate limit. This limit depends on the color used (the red sky is ~ 1 mag arcsec^{-2} brighter than the blue) and the size of the lowest contours, since this determines the signal-to-sky-noise ratio. In most cases, we measured isophotes down to a few percent of the sky brightness. In general, *B* and *R* magnitudes were not available for the objects, and it was necessary to estimate one (or both) assuming standard QSO and galaxy colors, knowing the approximate proportions of each. This process converges to the magnitudes given in Table 1. Where magnitudes are estimated, they are in parentheses in Table 1. Corrections were made to the L_N/L_F ratio and absolute magnitudes as given in the preceding section.

The distributions of the L_N/L_F ratios are shown in Figure 5. Values range over three orders of magnitude, with overall geometric mean 2.0 ± 1.2 in *R*. Subsidiary peaks in *R* appear at 0.25, 1.0, and 4. In *B*, the distribution is flatter, covering the same range. The *R* values are more likely to refer to the galaxy than the *B*, since the latter may be strongly affected by regions of recent hot star formation (Paper III) unrelated to the galaxy's undisturbed older population. The mean *B* ratio value is higher than the *R*, consistent with the nucleus being bluer than the galaxy. The radio-loud objects have more high L_N/L_F values, which is consistent with the fact that they are also optically more luminous objects (Fig. 5).

The correlation between L_N/L_F and QSO color is shown in Figure 6. The objects dominated by nuclear luminosity are blue, whereas those where the galaxy is brighter are red. While this is to be expected, it gives us confidence in the data reduction procedures used. Further, we can now understand to first order why QSOs have different colors, and that the simplest type of data (*UBV* photometry) can tell us something about the relative brightness of the QSO and its host galaxy. Objects whose colors are much redder than ~ 1.0 must be intrinsically reddened. At very high redshifts the nuclear colors themselves become red due to *K*-corrections.

The lowest L_N/L_F values generally are found in the lowest redshift objects ($z < 0.1$). This is simply because the intrinsically less luminous objects are more easily found when they are close. Beyond $z \sim 0.1$ there is no correlation of

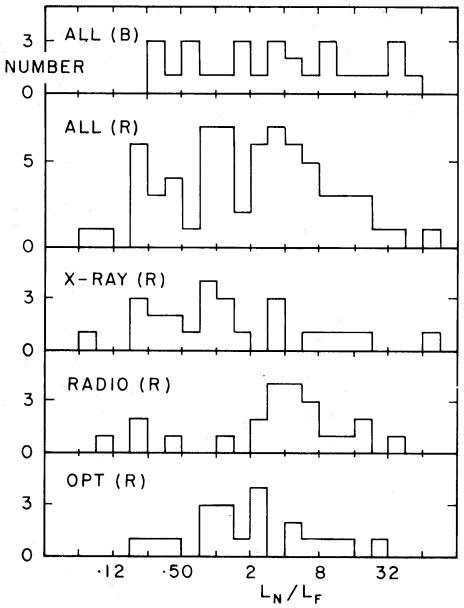

FIG. 5.—Histograms of corrected L_N/L_F ratios by discovery type in red, and for whole sample in blue and red.

L_N/L_F with redshift, with a *R*-band geometric mean of 2.5 ∓ 1.2. It seems unlikely that L_N/L_F evolves only for $z < 0.1$.

b) Absolute Magnitudes

The luminosities of the host galaxies range over ~ 7 mag, while those of the nuclei range over ~ 9 mag. There is a good correlation between them, as shown in Figure 7. Brighter QSOs lie in brighter galaxies. Linear regression fits in both *B* and *R* indicate that the nuclear magnitude rises 60% faster than that of the galaxy. Discovery criteria may select against objects in the top left-hand part of the diagram, but the lower right-hand side is significantly empty and so the relations seen in Figure 7 *may* be lower bounds. However, the diagram strongly suggests that the nuclear power source is related to the galaxy mass.

Once again, we see that the radio-loud QSOs are more luminous and reside in more luminous galaxies. However,

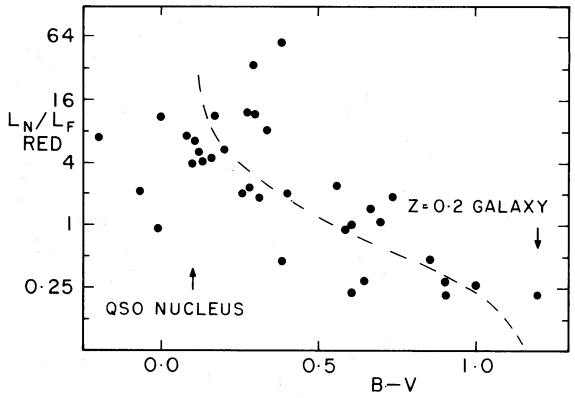

FIG. 6.—Ratio of nuclear to fuzz luminosity with QSO broad-band color. Dashed line is expected relation for $z \sim 0.2$ QSO. Arrows indicate nuclear and galaxy colors. General behavior of data follows expected relation. Plot does not include three objects of $B-V < -0.5$ and three of $B-V > 1.3$.

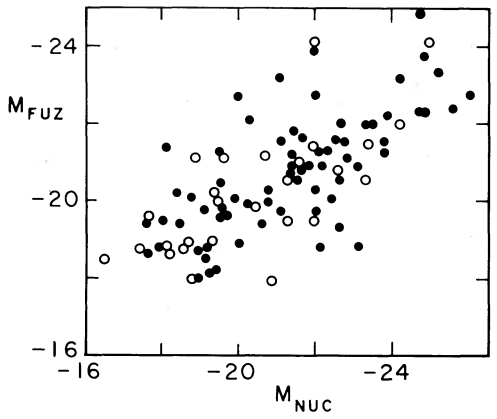

FIG. 7.—Relation between nuclear and host galaxy luminosity. Open points are blue; closed are red. Blue is shifted ~0.5 mag in M_{fuz} to higher luminosity. Correlation shows that brighter QSOs lie in brighter galaxies but that nuclear luminosity rises faster.

three similarly luminous optically selected PG objects (1216+069, 1425+267, 1700+518) have luminous host galaxies, so it is not clear that this difference is related to radio emission. On the other hand, these three objects *do* have appreciable radio emission (Kellerman and Gower, both private communications), so the question remains open for now.

Finally, we examine the relation between X-ray and radio luminosity. The nuclear optical and X-ray luminosities are directly proportional to each other in the mean (Fig. 8), so that (from Fig. 7) the galaxy luminosities rise more slowly than X-ray luminosities. This then suggests, as expected, that the X-ray luminosity originates in the nuclei of the QSOs. Radio nuclear luminosity, on the other hand, shows no correlation with the optical nuclear luminosity but does show a weak variation with the galaxy luminosity (Fig. 8). This interesting correlation, if real, may be a significant datum in understanding the radio emission phenomenon. The radio

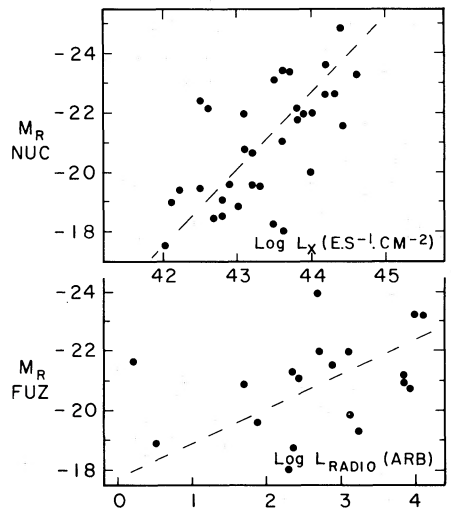

FIG. 8.—*Upper*, direct proportionality correlation between nuclear and X-ray luminosity. *Lower*, suggested linear correlation of nuclear radio luminosity and galaxy luminosity.

luminosity is not correlated with L_N/L_F or the luminosity of the nucleus. Numerous models postulate that some form of beaming mechanism is responsible for the visibility of radio emission. If this is true, then the lack of correlation with the nuclear luminosity implies that beaming cannot also be responsible for the optical brightness (at least, not beaming in the same direction).

V. ISOPHOTE AXIAL RATIOS AND SCALE LENGTHS

In Paper II we discussed the axial ratios of our outermost isophotes and compared the distribution with those of elliptical and spiral galaxies. It is now apparent that this was an oversimplification. In particular we find that several objects have the characteristics of barred spirals, in which the long axis of the isophote rotates through 90° in going through lower intensity levels. In others, the axial ratio becomes steadily smaller toward lower intensities, as it does for inclined disks. We therefore measured the axial ratios over as wide a range of intensity as they were possible, not just at the lowest level. Table 1 shows these values, at the designated intensity levels. Figure 9 shows histograms of the distribution at 23, 24, and 25 mag arcsec^{-2}. It is at once apparent that the distribution changes significantly with intensity level. The changes are attributable to a mixture of three types of object: barred types in which the ratio increases, sometimes through unity (the 90° rotation); the disk types in which it decreases; and a third type in which it remains the same at all levels. The former two types predominate, and their mean behavior as a function of intensity level is indicated in the figure by the dashed lines. It is clear that this qualitatively explains the gross changes in the distribution and that comparison with normal galaxies must be done with the same considerations in mind. We do note, however, that the principal two types and the third in which the axis ratio is small (<0.6) are all very characteristic of spiral, and not elliptical, galaxies.

Table 1 also shows scale lengths for resolved luminosity. These are determined from the slopes of the log I versus R plots, after subtraction of the point spread function to achieve the best linear residual. Only well determined values are given, and slopes are derived from data points for which the unresolved component is no more than ~50% of the observed intensity. The radius used is the azimuthal average, i.e., the radius of a circle whose area is equal to that of the isophote observed. No correction is made for ellipticity or assumed line-of-sight inclination. In some cases (specifically mentioned in Table 1 and the next section) a low-luminosity "halo" or filament is seen, whose scale length is much larger than that of the inner "galaxy." We have been careful to separate these from the main scale length measures—a point not fully attended to in Paper II.

In a number of cases, there were other resolved objects in the vicinity of the QSO, and, where possible, scale lengths were measured for these too. In almost all cases, log I of these objects falls off linearly with radius and the slopes are well defined.

A striking result is that in many cases we find that the nearby objects to QSOs have essentially the same scale length in red light. In the blue, the scatter is larger and there are far fewer observed comparisons. In the ~30 cases where scale lengths of QSO and neighboring objects were compared,

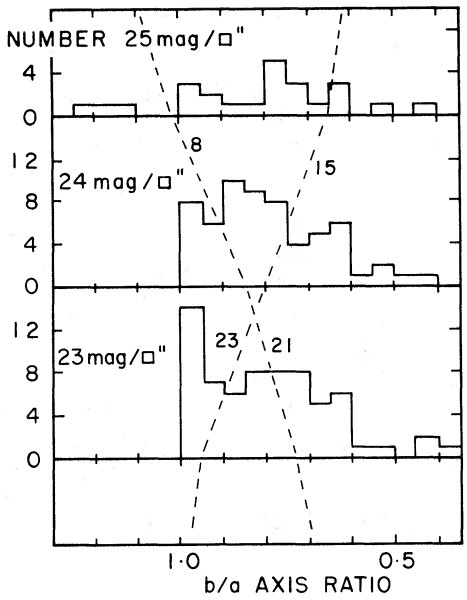

FIG. 9.—Axial ratio histograms of QSO galaxies at three intensity levels. Dashed lines show how two principal types behave. Numbers show how many observed objects behave in this way over each interval. Histogram changes are principally correlated with these, which are considered to correspond to inclined disk and barred spiral systems.

57% differed by less than 10%, and 77% by less than 20%. In a number of cases we know from redshift measures or galaxy counts that the nearby objects are almost certainly at the same distance as the QSO. Conversely, in a few cases where we know the objects are not associated, the agreement in scale length is poor.

All resolved objects appear to have approximately the same scale length, 2.1 ± 0.1 kpc; $\sigma = 1.0$ kpc, virtually independent of any other parameters. Published surface photometry of nearby galaxies (e.g., Freeman 1970; Fraser 1977; Boroson 1981) reveals scale length dependence on a variety of parameters including Hubble type, luminosity, etc. Nevertheless, the (azimuthally averaged) scale lengths in V light of Fraser's (1977) sample of 48 Virgo Cluster galaxies have a mean of 2.1 kpc with a standard deviation of only 0.6 kpc (the scatter is larger in B). Two selection effects which combine to reduce the dispersion in scale lengths in *any* magnitude-limited sample of a cluster are (1) very luminous galaxies are rare, and (2) only the brightest cluster members were well observed. Similar selection effects apply to our sample of QSO "host galaxies" and companion galaxies. An additional small selection effect in our sample is due to our limited spatial resolution which precludes measurement of low scale lengths at high redshifts (no scale lengths less than 2 kpc for $z > 0.35$ were measured). Correction for this effect will make the distribution of scale lengths as a function of z a little less peaked than it appears in Figure 10, since the maximum is at ~ 1.8 kpc. We note, parenthetically, that measurement of scale lengths may be a good method of determining distances to galaxies, and, if redshifts are known as well, of investigating fundamental cosmological parameters.

There are no substantial differences among the distribution of scale lengths of optical, radio, or X-ray selected quasars (Fig. 10). A weak correlation exists in the expected sense between the scale lengths and the luminosity of the QSO host galaxy.

The agreement between the scale lengths of a QSO host galaxy and a companion galaxy appears therefore to be evidence that they are at the same distance. On this basis, we have designated neighboring objects to QSOs as true companions if their R scale lengths agree to within 20%. As for the L_N/L_F ratios, the larger scatter in B light may be due to effects of a high rate of star formation as a result of tidal interactions or QSO activity and be less related to the underlying mass distribution of the galaxy.

There are two objects (1606+291 and 2206−197) whose scale lengths and luminosities are anomalously low if their redshifts are correct as published. Both are optically selected quasars with redshifts derived from objective prism spectra. Such estimates can easily be in error, and so we have arbitrarily adopted higher redshift values for these objects which bring their luminosities, L_N/L_F ratios, and scale lengths into better agreement with these quantities for the whole sample. The redshifts of these two objects should be remeasured.

The fact that we have chosen to measure all QSO galaxies as if they are exponential does not necessarily imply that they do not fit an $r^{-1/4}$ law as well. As noted in Paper I, it is impossible to differentiate between the two models, even for our best data, by varying the intensity of the point spread functions subtracted. In no case does the $r^{-1/4}$ law fit better than an exponential, with the possible exception of 1351+690. In view of the uncertainty in any conclusions based on such fits, we have not used them to say anything about the underlying galaxy type of morphology. We do stress the good agreement between QSO scale lengths and companions, with good exponential behavior, and refer to the next section for other indicators of galaxy type.

There is an additional minor point on scale lengths. A few

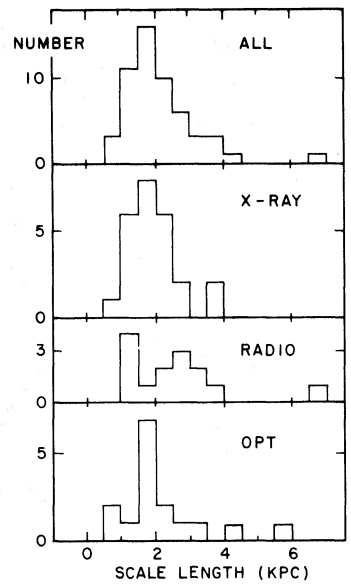

FIG. 10.—QSO galaxy scale length distribution. Note strong peak near 2 kpc. Resolution effects will cause these to lose ~10% of points <2 kpc.

QSO companions have smaller scale lengths than the host galaxy of the QSO in spite of evidence that they are associated. In all these cases, however, this occurs where there is strong evidence for an interaction between QSO and companion, and the implication is that the interaction has disturbed or stripped the fainter galaxy so that its morphology has been drastically altered (see also Stockton 1982).

VI. GALAXY MORPHOLOGY, INTERACTIONS, AND GROUPS

The most important morphological information is the presence of spiral structure. At large redshifts we are clearly limited in this respect, and one of the significant tests is the difference between blue and red images, which may trace the hot star population. In a number (seven) of QSOs we find clear barred spiral structure, as mentioned earlier. In eight more we see spiral structure in the blue-red images. There are 11 more cases where these kinds of evidence are less certain, but very suggestive, mainly because they are less well resolved, i.e., at higher redshift. In all 11 cases the entire galaxy is either very elongated or very irregular, even if we are not certain of the detailed structure. In a further eight cases we see a very irregular galaxy. Since even irregularity is characteristic of spirals and not of ellipticals, we count these (with varying weight) a spiral type. The remaining 41 galaxies have no significant morphological information, principally because they are insufficiently resolved, or in some cases because no features can be detected in them. The reader is referred to the detailed maps and comments, to be published separately (Hutchings *et al.* 1984).

Three of our objects (0851+202, 0957+227, and 1400+162) are BL Lac objects. We find no evidence that their host galaxies are different from other objects in the sample, or that they are similar to each other. In particular, we stress that for the redshifts adopted, the host galaxies in the two resolved cases do not have the luminosity of a giant elliptical. Therefore we stress that in our work we find no evidence for the prevalent assumption that BL Lac objects are in E galaxies.

There are six cases in our sample in which the QSO galaxy is clearly in the process of interaction with another galaxy. Most of these have been described in Papers III and IV. The main criteria for claiming interaction are overlap of isophotes, connected disturbance of symmetry, redshift correspondence, and connecting luminosity above the lowest isophote levels in other directions. We have 15 more cases which are less certain but very probable interactions, and a further seven where the evidence is of lower quality but still very suggestive. Once again, the evidence is usually poorer in the higher redshift cases where apparent luminosities are lower and resolution is poorer. The distribution of all 28 interacting cases is very uniform in both redshift and luminosity. The strongest cases, naturally, all lie at lower redshifts ($z < 0.2$). A further seven objects have close companions (within 15″, with the same scale length and/or redshift) which show no evidence for current interaction. In addition to these, a further 21 objects lie in groups or clusters of more than four objects including the QSO. This is not the result of a systematic or complete search, but simply the most obvious cases, where several galaxies lie within ~20″ of the QSO, with the same scale length, or there is a larger-scale clustering of galaxies including the QSO. The latter case—of clustering—occurs in four instances, involving six QSOs, and all are confirmed by other independent work. They are 1641+399a,b (Margon, Chanan, and Downes 1981), 1400+612 (Weistrop *et al.* 1983), 2217+08 NE (Harris *et al.* 1983), and 2251−178a,b (Kriss and Canizares 1982). Once again, more details on individual sources are given separately.

TABLE 2

QSO GALAXY MORPHOLOGICAL SUMMARY

Parameter	Total	Radio	X-Ray	Optical
Number	78	26	29	23
Spiral galaxy	35%	4%	55%	43%
Probable spiral	45%	12%	59%	67%
Type unknown	47%	77%	38%	26%
Interacting	8%	8%	10%	5%
Probable interacting	28%	35%	31%	17%
Possible interacting	37%	46%	45%	17%
Interacting or close companion	47%	54%	52%	30%
Group or cluster	26%	35%	28%	19%
Halo	17%	15%	21%	17%
Filaments or jets	12%	8%	10%	22%

Two other morphological features found in some objects are the outer extended halos mentioned earlier, and narrow features like filaments or jets which are clearly not part of the main QSO galaxy by reason of their size or extreme asymmetry. Halos are seen in 11 objects and in many cases are one-sided or double-tailed (like tailed radio sources), suggesting interaction with a medium or possibly the aftermath of an interaction with another galaxy. Filaments and jets are seen in eight objects and may also be results of tidal encounters.

A summary of the morphological findings is given in Table 2. We note once again the similarities among objects of all discovery types. Possible exceptions here are a lack of spiral characteristics in radio objects, although this is entirely consistent with the higher percentage of poorly resolved cases in this group due to their larger redshift (0.31 average compared with 0.15 and 0.18 for the others). The other possible exception is that fewer optically selected objects are interacting or in groups. However, these differences are based on very small numbers and are only marginally significant.

The overall conclusion is the same as that of Paper IV: that very large fractions (30–40%) of the sample have spiral characteristics, are interacting, and are in groups or small clusters of galaxies. The results strongly support the interaction hypothesis for triggering QSO activity. (See Paper IV, De Roberts 1983, and Stockton 1982 for further discussion.)

A last point to investigate is the few objects we did not resolve. Are these anomalous and therefore interesting, or is there a more mundane reason? In several cases, the latter is true (low plate limits, wrong published z), and in others we may wonder if the QSOs themselves are strongly beamed (OJ 287) or in stripped galaxies. Further work should be done on these objects in case they are important.

VII. CONCLUSIONS

Our data on 78 QSOs suggest that all QSOs reside in galaxies of average to high luminosity, and that the most

energy source is an accretion-limited black hole, this may imply that its mass is related to that of the galaxy, increasing 60% faster than that of the galaxy, if mass and luminosity are directly proportional in both. The evidence suggests that QSOs normally reside in spiral galaxies, in agreement with Boroson, Oke, and Green (1982), and that interactions or gross disturbances of the galaxies are almost certainly connected with the QSO phenomenon. The proportion of interacting galaxies in our sample is more than an order of magnitude higher than that expected for random local galaxies (De Robertis 1983). The data support the suggestion (Papers III and IV; De Robertis 1983) that QSOs are powered by encounters which perturb gas into the galactic nucleus and activate it. The scarcity of twin QSOs in such a scenario can result from (*a*) absence of a massive black hole in many galactic nuclei and (*b*) a one-sidedness of the gas stripping in such encounters. Our data are consistent with other findings (e.g., Yee and Green 1984; French and Gunn 1983) that QSOs reside in dense groups of galaxies, in which such encounters are very probable. We have two cases of two luminous QSOs lie in the brightest galaxies. If the central QSOs in a cluster of galaxies, suggesting that larger clusters are also favorable environments for QSO activity.

If we ask whether we should not see these cluster pairs more frequently, we note that the second object in each of the two cases is a few magnitudes fainter, and was discovered by X-ray rather than optical radiation. Thus pairs may well exist, but be hard to find because one of them is faint and X-ray surveys are very incomplete. A search for QSOs in clusters at larger redshifts would be an important step in advancing the interacting hypothesis.

The nuclear to galaxy luminosity ratios extend from typical Seyfert values of 0.1 to a factor 50 or more, emphasizing the continuity of the phenomenon through a wide luminosity range. An important parallel to this work is clearly the spectroscopic investigation of QSO galaxies and companions, to study their composition, association, and dynamics.

We thank the following colleagues for their advice, and data in advance of publication: Ann Gower, Paul Hintzen, John Kormendy, Jerry Kriss, Bruce Margon, and Harvey Tananbaum.

REFERENCES

Balick, B., and Heckman, T. 1983, *Ap. J.* (*Letters*), **265**, L1.
Boroson, T. A. 1981, *Ap. J. Suppl.*, **46**, 177.
Boroson, T. A., Oke, J. B., and Green, R. F. 1982, *Ap. J.*, **263**, 32.
Chanan, G. A., Margon, B., and Downes, R. A. 1981, *Ap. J.* (*Letters*), **243**, L5.
———. 1983 preprint.
De Robertis, M. M. 1983, preprint.
Fraser, C. W. 1977, *Astr. Ap.*, **29**, 161.
Freeman, K. C. 1970, *Ap. J.*, **160**, 811.
French, H. B., and Gunn, J. E. 1983, *Ap. J.*, **269**, 29.
Gezari, D. Y., Schmitz, M., and Mead, J. M. 1982, NASA Tech. Memo 83819.
Gower, A. C. 1983, private communication.
Grindlay, J. E., *et al.* 1980, *Ap. J.* (*Letters*), **239**, L43.
Harris, D. E., Dewdney, P. E., Costain, C. H., Butcher, H., and Willis, H. G. 1983, *Ap. J.*, **270**, 39.
Hewitt, A., and Burbidge, G. R. 1980, *Ap. J. Suppl.*, **43**, 57.
Hintzen, P., Ulvestad, J. S., and Owen, F. N. 1983, *A.J.*, **88**, 709.
Hutchings, J. B., and Campbell, B. 1983, *Nature*, **303**, 584 (Paper IV).
Hutchings, J. B., Campbell, B., and Crampton, D. 1982, *Ap. J.* (*Letters*), **261**, L23 (Paper III).
Hutchings, J. B., Crampton, D., Campbell, B., Duncan, D., and Glendenning, B. 1984, *Ap. J. Suppl.*, **280**, in press.
Hutchings, J. B., Crampton, D., Campbell, B., Gower, A. C., and Morris, S. C. 1982, *Ap. J.*, **262**, 48 (Paper II).
Hutchings, J. B., Crampton, D., Campbell, B., and Pritchet, C. 1981, *Ap. J.*, **247**, 743 (Paper I).
Kriss, G. A. 1982, thesis, MIT.
Kriss, G. A., and Canizares, C. R. 1982, *Ap. J.*, **261**, 51.
Margon, B., Chanan, G. A., and Downes, R. A. 1981, *Nature*, **290**, 480.
Margon, B., *et al.* 1983, preprint.
Sandage, A. R. 1972, *Ap. J.*, **178**, 1.
———. 1973, *Ap. J.*, **183**, 711.
Stockton, A. 1982, *Ap. J.*, **257**, 33.
Tananbaum, H. 1982, private communication.
Tyson, J. A., Baumm, W. A., and Kreidl, T. 1982, *Ap. J.* (*Letters*), **257**, L1.
Weistrop, D., Shaffer, D. B., Reitsema, H. J., and Smith, B. A. 1983, *Ap. J.*, **271**, 471.
Wyckoff, S., Wehinger, P., and Gehren, T. 1981, *Ap. J.*, **247**, 750.
Wyckoff, S., *et al.* 1983, in *Quasars and Gravitational Lenses* (*Univ. de Liège*), p. 483.
Yee, H., and Green, R. F. 1984, *Ap. J.*, **280**, in press.
Zamorani, G., *et al.* 1981, *Ap. J.*, **245**, 357.

B. CAMPBELL, D. CRAMPTON, and J. B. HUTCHINGS: Dominion Astrophysical Observatory, 5071 W. Saanich Road, Victoria, B.C., V8X 4M6, Canada